

Time-Varying Bandpass Filter Based on Assisted Signals for AM-FM Signal Separation: A Revisit*

Guanlei Xu¹, Xiaotong Wang², Xiaogang Xu², Lijia Zhou¹, Limin Shao¹

¹Ocean Department of Dalian Naval Academy, Dalian, China; ²Navigation Department of Dalian Naval Academy, Dalian, China.
Email: xgl_86@163.com

Received June 2nd, 2013; revised July 5th, 2013; accepted July 13th, 2013

Copyright © 2013 Guanlei Xu *et al.* This is an open access article distributed under the Creative Commons Attribution License, which permits unrestricted use, distribution, and reproduction in any medium, provided the original work is properly cited.

ABSTRACT

In this paper, a new signal separation method mainly for AM-FM components blended in noises is revisited based on the new derived time-varying bandpass filter (TVBF), which can separate the AM-FM components whose frequencies have overlapped regions in Fourier transform domain and even have crossed points in time-frequency distribution (TFD) so that the proposed TVBF seems like a “soft-cutter” that cuts the frequency domain to snaky slices with rational physical sense. First, the Hilbert transform based decomposition is analyzed for the analysis of nonstationary signals. Based on the above analysis, a hypothesis under a certain condition that AM-FM components can be separated successfully based on Hilbert transform and the assisted signal is developed, which is supported by representative experiments and theoretical performance analyses on a error bound that is shown to be proportional to the product of frequency width and noise variance. The assisted signals are derived from the refined time-frequency distributions via image fusion and least squares optimization. Experiments on man-made and real-life data verify the efficiency of the proposed method and demonstrate the advantages over the other main methods.

Keywords: Time-Varying Bandpass Filter (TVBF); Hilbert Transform; Assisted Signal; AM-FM Component; Time-Frequency Distribution (TFD)

1. Introduction

The decomposition of signals blended in noises is a real-life problem in measurement and other signal processing fields, which includes two tasks: first filtering and then decomposing the signals. The filtering of signals from observed noisy data, while preserving their original features respectively, remains a challenging problem in both signal processing and statistics. A number of filtering methods have been proposed, particularly for the case of additive white Gaussian noise [1-10]. Frequently, linear methods such as the Wiener filtering [1,4,10,11] are used because linear filters are easy to design and implement. However, linear filtering methods are not very effective when signals are nonstationary. To overcome the shortcomings, nonlinear methods have been proposed such as wavelet thresholding [5,7]. The idea of wavelet thresholding relies on the assumption that signal magnitudes dominate the magnitudes of the noise in a wavelet representation so that wavelet coefficients can be set to zero if

their magnitudes are less than a predetermined threshold [1,7]. A limit of the wavelet approach is that the basic functions are fixed and, thus, do not necessarily match all real signals. On the other hand, the second task—the decomposition of multi-components is also an important problem in signal processing. The adaptive methods for signal separation should be explored [2,8-18] especially for the separation of multiple components blended in noise data. That is to say, the separation of signals from real-life observed noisy data includes two steps’ work, filtering the signals and then decomposing the signals to multiple independent components. In most of the reported papers [1-25], the two tasks are separate and they cannot do the both tasks at the same time. In this paper, we will combine these two tasks to single one.

Among many types of signals, the AM-FM (amplitude modulation and frequency modulation) signals are one of the most important ones and play an important role in various signal processing fields [1]. In telecommunications, amplitude modulation and frequency modulation convey information over a carrier wave by varying its instantaneous amplitude and frequency. AM-FM signals

*This work was fully supported by the NSFC (61002052) and partly supported by the NSFCs (61250006 and 60975016).

are also widely used in telemetry, radar, seismic prospecting and newborn EEG seizure monitoring, broadcasting music and speech, two-way radio systems, magnetic tape-recording systems and some video-transmission systems. Furthermore, many real-life signals can also be taken as the AM-FM signals approximately. In some cases, once the multiple AM-FM components are superposed and noised, the information carried by every AM-FM component is blended and hidden and cannot be recognized clearly. In this work, an elementary fundamental problem how to separate the AM-FM components blended in noises is addressed.

There have been some methods involving decomposing the superposed AM-FM components, including the frequency domain separation method such as the LFM (linear frequency modulation) component separation via FRFT [17], the empirical mode decomposition (EMD) [3,12], the improved EMD (IEMD) [2,8] (the method in [8] is only for pure FM signal), the masking method [13,14] and the Hilbert transform [1,19] based method [16]. The frequency domain separation method is the most traditional method to separate the superposed AM-FM components in frequency domain or fractional frequency domain [17] through finding the separation points or peak points. For the case that the superposed AM-FM components have distinguishable frequency regions, the separation is done well. Unfortunately, once the superposed AM-FM components have overlapped and undistinguishable frequency regions, the separation method in frequency domain will fail to work.

After the introduction of the HHT by Huang *et al.* [12], the EMD has become an important tool to analyze nonlinear and non-stationary signals by breaking them down into a number of elementary amplitude and frequency modulated (AM/FM) zero mean signals termed intrinsic mode functions (IMFs). The EMD can separate the superposed AM-FM components successfully under some conditions that have been addressed by Rilling and P. Flandrin [18], *i.e.*, when and where the two tones (can be taken as two simple AM-FM components) can be separated well using EMD. If these conditions are not satisfied, EMD fails to separate them. Therefore, the improved EMD (IEMD) method [2] for AM-FM component decomposition is proposed in order to avoid the failure of EMD. Although IEMD can improve the performance, there are still some problems. First, the IEMD method is not stable, and in some cases it fails to separate the superposed AM-FM components, *e.g.*, the possible failure of the polynomial estimation for more complicated frequency and phase functions due to the long signal's length. Second, the employment of this IEMD method is cumbersome for more complicated cases such as the components with crossed instantaneous frequencies.

The masking method [13,14] uses the mask signals to help decompose the superposed AM-FM components. In fact this method makes full use of the characters of filter bank for EMD [3] to extract the component whose frequency is close to the mask signal, and then eliminates the mask signal in IMFs to obtain the components. This method has two problems. The mask signal is based on Fourier spectral, therefore this method fails to handle the case of time-varying instantaneous frequencies that have overlapped frequency regions in frequency domain. In addition, this method still fails to separate two components with crossed frequencies.

Differently, the Hilbert transform based method can separate the superposed AM-FM components whose frequencies are very close in principle. Unfortunately, the frequency of the assisted signal used in the Hilbert transform based method needs to be found in the Fourier transform domain via the valley values that can distinguish the different frequency modes. In other words, in the case of more overlapping of frequencies, this method will fail.

In this paper, we will first analyze the performance of the Hilbert transform based method in great details and find its limitation, and then find its potential value for analysis of the more complicated cases such as time-varying instantaneous frequencies with overlapped and crossed points. The main aim in Section 2 to analyze the Hilbert transform based method is twofold: 1), we want to know what amplitudes and frequencies are the optimal for the assisted signals; 2), for the overlapped frequencies (*e.g.*, the **Figure 1**) in Fourier transform domain, whether this method will still work well or not? After that, in Section 3, the time-varying bandpass filter based on Hilbert transform and assisted signals is proposed, in addition the error bounds are analyzed theoretically and verified via simulations. The estimation of time-varying assisted signals is addressed in Section 4 via image fusion and least square optimization. In Section 5 experiments on man-made and real-life data are shown. Section 6 concludes this paper.

2. Component Separation via Hilbert Transform and Assisted Signal

2.1. Component Separation

The decomposition theorem [16] by G. Chen and Z. Wang is defined as follows. Let $x(t)$ denote a real time series of n significant frequency components $(\omega_1, \omega_2, \dots, \omega_n \geq 0)$ in $L^2(-\infty, +\infty)$ of the real time variable t . It can be decomposed into n signals $x_i^{(d)}(t)$ ($i = 1, 2, \dots, n$) whose Fourier spectra are equal to $X(\omega)$ over n mutually exclusive frequency ranges:

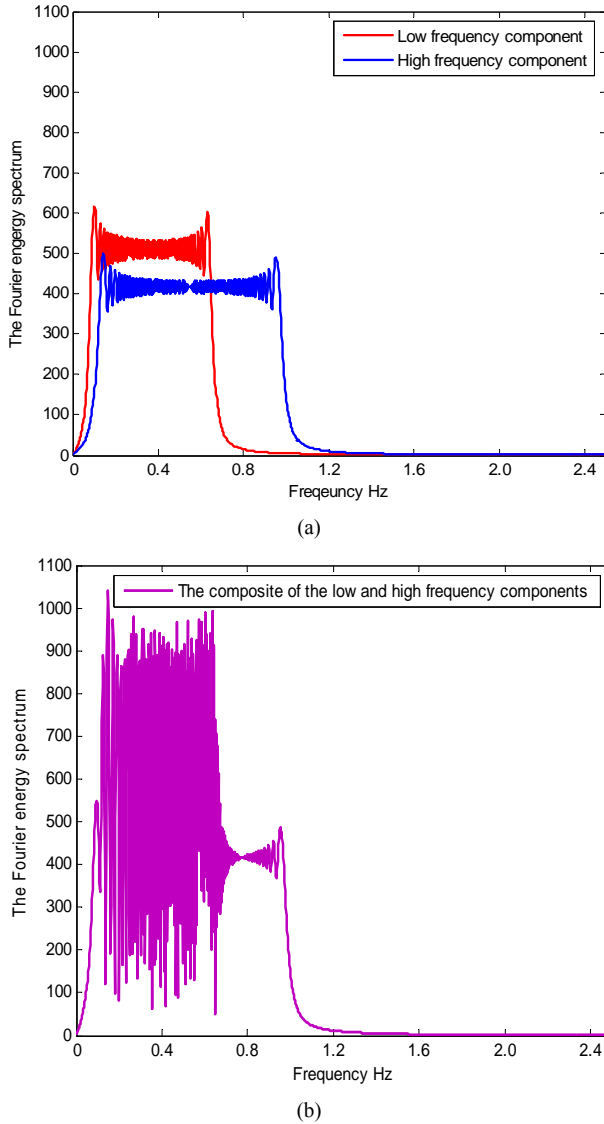


Figure 1. An example of two AM-FM components that can be separated successfully via Equations (6) and (7). Here $x_1(t) = \cos(2\pi(0.12t + 1)t)$, $x_2(t) = \cos(2\pi(0.18t + 1.5)t)$ and $x_{as,cos}(t) = \cos(2\pi(0.15t + 1.25)t)$, $x_{as,sin}(t) = \sin(2\pi(0.15t + 1.25)t)$. Sampling frequency is 500 Hz, time support is 30 seconds. Finally, $er < 0.001$.

$[0, \omega_{as,1}), (\omega_{as,1}, \omega_{as,2}), \dots, (\omega_{as,n-1}, \omega_{as,n})$. That is,

$$x(t) = \sum_{i=1}^n x_i^{(d)}(t). \quad (1)$$

Here, $X(\omega)$ is the Fourier transform of $x(t)$, ω represents a frequency variable, and $\omega_{as,i} \in (\omega_i, \omega_{i+1})$ ($i=1, 2, \dots, n$) are $n-1$ assisted frequencies for the assisted signals. Each signal has a narrow bandwidth in the frequency domain and can be determined by

$$x_i^{(d)} = s_i(t) - s_{i-1}(t), \dots, x_n^{(d)} = x(t) - s_{n-1}(t), \quad (2)$$

$$s_i(t) = \sin(\omega_{as,i}t) \cdot H\{x(t) \cdot \cos(\omega_{as,i}t)\} - \cos(\omega_{as,i}t) \cdot H\{x(t) \cdot \sin(\omega_{as,i}t)\}, \quad (3)$$

where $s_0(t) = 0$, and $H\{\cdot\}$ represents the Hilbert transform of the function inside the bracket “ $\{\cdot\}$ ”.

The proof of this theorem can be found in [2]. This theorem tells us two key issues: the determination of assisted signal and the condition that this theorem holds. Very fortunately we find an exciting fact: even if there are overlapped frequency ranges in Fourier transform domain, the above theorem still hold in some conditions.

Hypothesis 1: For two harmonic AM-FM components $x(t) = x_1(t) + x_2(t)$ ($x_1(t) = a_1 \cos(\omega_1(t)t)$ and

$x_2(t) = a_2 \cos(\omega_2(t)t)$) in $L^2(-\infty, +\infty)$, if

$\omega_2(t) > \omega_{as}(t) > \omega_1(t) > 0$ and a_1, a_2 are positive amplitudes, it's possible we have

$$x_1(t) = \sin(\omega_{as}(t)t) \cdot H\{x(t) \cdot \cos(\omega_{as}(t)t)\} - \cos(\omega_{as}(t)t) \cdot H\{x(t) \cdot \sin(\omega_{as}(t)t)\}, \quad (4)$$

$$x_2(t) = x(t) - x_1(t), \quad (5)$$

if $\omega_2(t), \omega_{as}(t), \omega_1(t)$ and a_1, a_2 satisfy certain conditions. These conditions will be determined by rational simulations in the following section.

2.2. The Conditions for Hypothesis 1

For two harmonic AM-FM components

$x_1(t) = a_1 \cos(\omega_1(t)t)$ and $x_2(t) = a_2 \cos(\omega_2(t)t)$

($x(t) = x_1(t) + x_2(t)$) in $L^2(-\infty, +\infty)$, we first assume

that $\omega_2(t) > \omega_{as}(t) > \omega_1(t) > 0$ and a_1, a_2 are positive

amplitudes. In order to simplify our analysis, we let

$x_1(t) = \cos(2\pi f(t)t)$, $x_2(t) = a \cos(2\pi cf(t)t)$ and

the assisted signal $x_{as,cos}(t) = \cos(2\pi kf(t)t)$,

$x_{as,sin}(t) = \sin(2\pi kf(t)t)$. Here $\omega(t) = 2\pi f(t) > 0$, the

circle instantaneous frequency $f(t)$ is slow-varying in $t \in R^+$, a, c and k are constants with $1 < k < c$. Then we can obtain

$$\tilde{x}_1(t) = x_{as,sin}(t) \cdot H\{x(t) \cdot x_{as,cos}(t)\} - x_{as,cos}(t) \cdot H\{x(t) \cdot x_{as,sin}(t)\} \quad (6)$$

$$\tilde{x}_2(t) = x(t) - \tilde{x}_1(t). \quad (7)$$

If $\tilde{x}_1(t) = x_1(t)$ and $\tilde{x}_2(t) = x_2(t)$, then the separation is fully successful, otherwise, there is error. To mea-

sure the error quantitatively, we set

$$er = \min \left(1, \max_{l=1,2} \left(\frac{\|x_l(t) - \tilde{x}_l(t)\|_{L^2(R)}^2}{\|x_l(t)\|_{L^2(R)}^2} \right) \right). \quad (8)$$

Clearly, if $er = 0$, then the separation is fully successful. With the increasing of er , the performance of decomposition will degrade. If $er = 1$, then the decomposition is a full failure.

2.2.1. For $k = \frac{c+1}{2}$ with a and c Varying

Case 1: the amplitude a changes from 10^{-6} to 10^6 , and c changes from 1 to 500 and $f(t) = 1$. The decomposition result can be found in **Figure 2(a)**.

Case 2: the amplitude a changes from 10^{-6} to 10^6 , and c changes from 1 to 500 and $f(t) = 0.05t + 1$. The decomposition result can be found in **Figure 2(b)**.

Case 3: the amplitude a changes from 10^{-6} to 10^6 , and c changes from 1 to 500 and $f(t) = 0.01t^2 + 0.02t + 1$. The decomposition result can be found in **Figure 2(c)**.

Clearly, for different instantaneous frequencies (the constant frequency, the linear modulation frequency and the quadratic modulation frequency), the decompositions are the similar and we can obtain the same result: if the amplitude a and the frequency ratio c are in the blue regions in the shape of ‘‘U’’, i.e., satisfy the relation

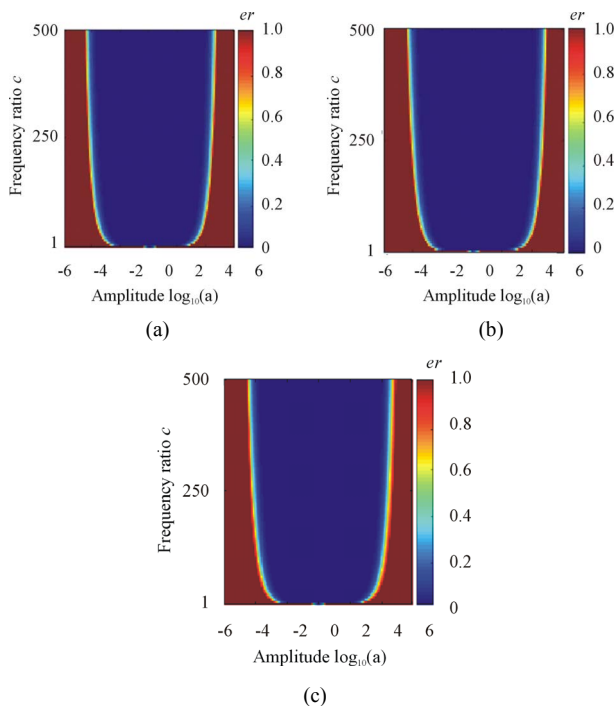


Figure 2. The separation results of different instantaneous frequencies via Equations (6) and (7).

$c \geq 4^{\lceil \log_{10} a \rceil}$, then the decomposition will be nearly perfect.

2.2.2. For $c = 2$ with a and k Varying

Case 1: the amplitude a changes from 10^{-6} to 10^6 , and k changes from 1 to 500 and $f(t) = 1$. The decomposition result can be found in **Figure 3(a)**.

$$x_1(t) = \cos(2\pi(0.12t + 1)t),$$

$$x_2(t) = \cos(2\pi(0.18t + 1.5)t) \text{ and}$$

$$x_{as,cos}(t) = \cos(2\pi(0.15t + 1.25)t),$$

$$x_{as,sin}(t) = \sin(2\pi(0.15t + 1.25)t).$$

Sampling frequency is 500 Hz, time support is 30 seconds. Finally, $er < 0.001$.

Case 2: the amplitude a changes from 10^{-6} to 10^6 , and k changes from 1 to 500 and $f(t) = 0.05t + 1$. The decomposition result can be found in **Figure 3(b)**.

Case 3: the amplitude a changes from 10^{-6} to 10^6 , and k changes from 1 to 500 and $f(t) = 0.01t^2 + 0.02t + 1$. The decomposition result can be found in **Figure 3(c)**.

Clearly, for different instantaneous frequencies (the constant frequency, the linear modulation frequency and the quadratic modulation frequency), the decompositions are the similar and we can obtain the same result: if the amplitude a and the frequency ratio k are in the blue regions, i.e., the middle region between the two functions

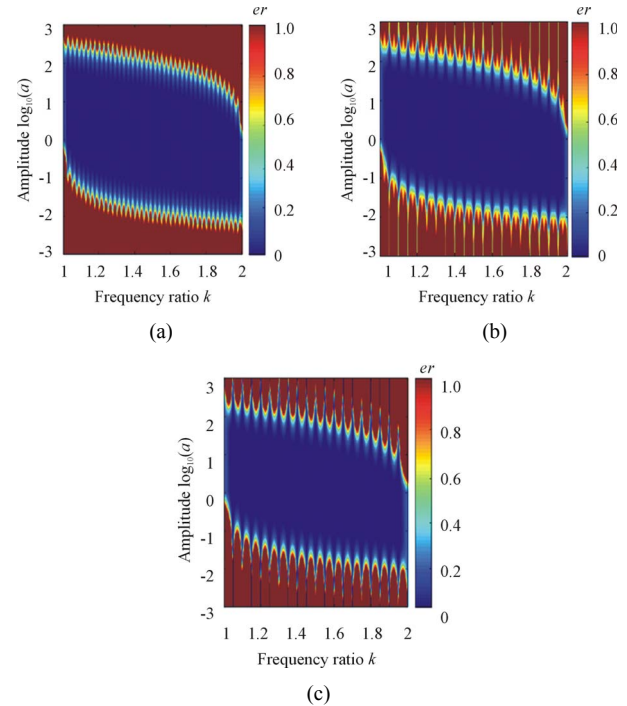


Figure 3. The separation results of different instantaneous frequencies via Equations (6) and (7).

$k = -\frac{(\log_{10} a)^2}{4} + 2$ and $k = 2(\log_{10} a)^2$, then the decomposition will be nearly perfect.

Therefore, if the amplitudes and frequencies of the two AM-FM components are known, the assisted signal's frequency can be selected in wide scope according to the above results because the conditions ($c \geq 4^{|\log_{10} a|}$, the middle region between $k = -\frac{(\log_{10} a)^2}{4} + 2$ and $k = 2(\log_{10} a)^2$) are very loose and easy to satisfy in practice.

The example in **Figure 1** is a breakthrough of the decomposition theorem in [16]. The simulations in **Figures 2** and **3** verify that this breakthrough is rational and find the performance bounds for the separation of two AM-FM components.

Compared with the performance limitation of EMD [12], the method based on Hilbert transform and assisted signal is a great improvement for component separation. That is, if we can obtain the rational assisted signals, the separation of AM-FM components will be feasible in principle.

3. Time-Varying Bandpass Filter

3.1. Time-Varying Bandpass Filter

Let $x(t) = \sum_{l=1}^3 x_l(t)$ with $x_l(t) = a_l \cos(\omega_l(t)t)$ denote a real time series of 3 significant instantaneous frequencies (here the amplitude $a_l > 0$, and these slow-varying instantaneous frequencies satisfy

$\omega_1(t) > \omega_2(t) > \omega_3(t) \geq 0$ for any $t \in [0, T]$. Now we want to obtain the interested component $x_{in}(t) = x_2(t)$

out of $x(t)$. $(x_{as,\cos}^{(1)}(t), x_{as,\sin}^{(1)}(t))$ and $(x_{as,\cos}^{(2)}(t), x_{as,\sin}^{(2)}(t))$ are the assisted signal pairs so that $x_{as,\cos}^{(1)}(t) = \cos(\omega_{as}^{(1)}(t))$, $x_{as,\sin}^{(1)}(t) = \sin(\omega_{as}^{(1)}(t))$ with

$$\omega_1(t) > \omega_{as}^{(1)}(t) > \omega_2(t), \quad (9)$$

$x_{as,\cos}^{(2)}(t) = \cos(\omega_{as}^{(2)}(t))$, $x_{as,\sin}^{(2)}(t) = \sin(\omega_{as}^{(2)}(t))$ with

$$\omega_2(t) > \omega_{as}^{(2)}(t) > \omega_3(t). \quad (10)$$

Then we can obtain an approximation of the interested component $x_{in}(t)$ with error δ by the **time-varying bandpass filter (TVBF)**

$$\begin{aligned} \tilde{s}_1(t) &= x_{as,\sin}^{(1)}(t) \cdot H \left\{ x(t) \cdot x_{as,\cos}^{(1)}(t) \right\} \\ &\quad - x_{as,\cos}^{(1)}(t) \cdot H \left\{ x(t) \cdot x_{as,\sin}^{(1)}(t) \right\}, \end{aligned} \quad (11)$$

$$\begin{aligned} \tilde{s}_2(t) &= x_{as,\sin}^{(2)}(t) \cdot H \left\{ x(t) \cdot x_{as,\cos}^{(2)}(t) \right\} \\ &\quad - x_{as,\cos}^{(2)}(t) \cdot H \left\{ x(t) \cdot x_{as,\sin}^{(2)}(t) \right\}, \end{aligned} \quad (12)$$

$$\tilde{x}_2(t) = \tilde{s}_1(t) - \tilde{s}_2(t), \quad (13)$$

where $0 \leq \delta = \frac{\|x_{in}(t) - \tilde{x}_2(t)\|_{L^2(T)}^2}{\|x_{in}(t)\|_{L^2(T)}^2} < 1$ (δ is a very small nonnegative value).

The most important is the selection of these functions $(\omega_{as}^{(1)}(t), \omega_{as}^{(2)}(t))$. In fact, if the instantaneous frequency $\omega_{in}(t) = \omega_2(t)$ is known, we can let $\omega_{as}^{(1)}(t) = (1 + \lambda)\omega_{in}(t)$ and $\omega_{as}^{(2)}(t) = (1 - \lambda)\omega_{in}(t)$ with $0 < \lambda < 1$ only if $\omega_1(t) > \omega_{as}^{(1)}(t) > \omega_{in}(t)$ and $\omega_{in}(t) > \omega_{as}^{(2)}(t) > \omega_3(t)$ hold. If the other two components $(x_1(t), x_3(t))$ are the noises (such as the zero-mean Gaussian white noises) whose bandwidths occupy the whole frequency domain. Therefore, we hope λ to be as small as possible. On the other hand, if λ is too small, the performance of TVBF in (11)-(13) will decrease because the limited signal resolution won't be too high for the reason of sampling and others. In the following section, we will address the optimal λ for fixed instantaneous frequency $\omega_{in}(t)$ under different SNR (signal-to-noise-ratio) (or noise variance σ).

3.2. Optimal Filter Parameter in Noises

In this section, we explore the optimal λ under different noise variance σ for the fixed instantaneous frequency $f_{in}(t)$ via simulations. We set

$x_{in}(t) = \cos(2\pi(0.002t^2 + 0.05t + 1)t)$ with the instantaneous frequency $f_{in}(t) = 0.002t^2 + 0.05t + 1$ (the time support $t \in [0, 30]$ and the sampling frequency is 500 Hz). According to (11)-(13), we set

$$x_{as,\cos}^{(1)}(t) = \cos(2\pi(1 + \lambda)f_{in}(t)t), \quad (14)$$

$$x_{as,\sin}^{(1)}(t) = \sin(2\pi(1 + \lambda)f_{in}(t)t),$$

$$x_{as,\cos}^{(2)}(t) = \cos(2\pi(1 - \lambda)f_{in}(t)t), \quad (15)$$

$$x_{as,\sin}^{(2)}(t) = \sin(2\pi(1 - \lambda)f_{in}(t)t).$$

Set $x(t) = x_{in}(t) + nn(t)$, and $nn(t)$ is the zero-mean Gaussian white noise with variance σ . Now we use the TVBF to obtain $\tilde{x}_{in}(t)$ (an approximation of the interested component $x_{in}(t)$) so as to see how the error δ varies while the variance σ and the parameter λ varying.

If there are no other components whose frequencies are close to the interested component, when the noise variance is small, we can let λ be large. However, if there are other components whose frequencies are close to the interested component, then we must let λ as small as possible. On the other hand, in order to separate the interested component, λ cannot be zero. Therefore, after analysis and simulation in **Figure 4** (see the red dot lines), we find that the optimal λ should be in the scope of $0.001 \sim 0.1$ in most cases. Of course, in practice we should take care of all the factors comprehensively to give a better choice of λ empirically.

Compared with the performance limitation of EMD [12], the method based on Hilbert transform and assisted signal is a great improvement for component separation. That is, if we can obtain the rational assisted signals, the separation of AM-FM components will be feasible in principle.

3.3. Performance Analysis in Noises

In follows, we will analyze the error resulted by the equivalent component that has the same frequency as the assisted signal pairs from the Gaussian noises and the mid-

$$x(t) = x_{in}(t) + mn(t) = x_{in}(t) + s_1(t) + s_2(t) + s_3(t) + s_4(t) + s_5(t). \quad (16)$$

Taking into account (14), (15) and (16), finally we obtain

$$\begin{aligned} \tilde{s}_1(t) &= x_{as,\sin}^{(1)}(t) \cdot H \left\{ x(t) \cdot x_{as,\cos}^{(1)}(t) \right\} - x_{as,\cos}^{(1)}(t) \cdot H \left\{ x(t) \cdot x_{as,\sin}^{(1)}(t) \right\} \\ &= \left\{ x_{in}(t) + s_3(t) + s_4(t) + s_5(t) \right\} + x_{as,\sin}^{(1)}(t) \cdot H \left\{ s_2(t) \cdot x_{as,\cos}^{(1)}(t) \right\} - x_{as,\cos}^{(1)}(t) \cdot H \left\{ s_2(t) \cdot x_{as,\sin}^{(1)}(t) \right\} \end{aligned}$$

Since the bandwidth of $s_2(t)$ is the same as $x_{as}^{(1)}(t)$ constant, we obtain $\|s_2(t)\| \ll \|x_{as}^{(1)}(t)\|$ so that and the Gaussian white noise's spectrum magnitude is

$$x_{as,\sin}^{(1)}(t) \cdot H \left\{ s_2(t) \cdot x_{as,\cos}^{(1)}(t) \right\} - x_{as,\cos}^{(1)}(t) \cdot H \left\{ s_2(t) \cdot x_{as,\sin}^{(1)}(t) \right\} \approx 0$$

without loss of generality, hence $\tilde{s}_1(t) \approx x_{in}(t) + s_3(t) + s_4(t) + s_5(t)$.

In the same manner, we have

$$\begin{aligned} \tilde{s}_2(t) &= x_{as,\sin}^{(2)}(t) \cdot H \left\{ x(t) \cdot x_{as,\cos}^{(2)}(t) \right\} - x_{as,\cos}^{(2)}(t) \cdot H \left\{ x(t) \cdot x_{as,\sin}^{(2)}(t) \right\} \\ &= s_5(t) + x_{as,\sin}^{(2)}(t) \cdot H \left\{ s_4(t) \cdot x_{as,\cos}^{(2)}(t) \right\} - x_{as,\cos}^{(2)}(t) \cdot H \left\{ s_4(t) \cdot x_{as,\sin}^{(2)}(t) \right\} \end{aligned}$$

Since the bandwidth of $s_4(t)$ is the same as $x_{as}^{(2)}(t)$ constant, we obtain $\|s_4(t)\| \ll \|x_{as}^{(2)}(t)\|$, so that and the Gaussian white noise's spectrum magnitude is

$$x_{as,\sin}^{(2)}(t) \cdot H \left\{ s_4(t) \cdot x_{as,\cos}^{(2)}(t) \right\} - x_{as,\cos}^{(2)}(t) \cdot H \left\{ s_4(t) \cdot x_{as,\sin}^{(2)}(t) \right\} \approx 0$$

without loss of generality, hence $\tilde{s}_2(t) \approx s_5(t)$.

Finally,

$$\begin{aligned} \tilde{x}_{in}(t) &\approx \tilde{s}_1(t) - \tilde{s}_2(t) \approx x_{in}(t) + s_3(t) + s_4(t) \\ &\approx x_{in}(t) + s_3(t) \end{aligned}$$

Taking into account that $s_3(t)$ is the equivalent component (coming from the Gaussian noise) whose band-

width occupies the frequency range between $(1+\lambda)f_{in}(t)$ and $(1-\lambda)f_{in}(t)$, and the Gaussian white noise's spectrum magnitude is constant, we get

$$\|\tilde{x}_{in}(t) - x_{in}(t)\| \approx \|s_3(t)\| \propto \lambda \cdot \sigma^2. \quad (17)$$

This implies that the recovery error is proportional to the value of λ and the variance σ^2 of the noise. This

has been verified by the simulation in **Figure 4** and the two results (the theoretical result in (17) and the simulation result in **Figure 4**) are consistent.

4. Parameter Estimation for Assisted Signals from TFDs

4.1. Refined TFD via Image Fusion

In order to obtain the assisted signals and their instantaneous frequencies, we need to obtain the refined TFD of the original signals in noises, in which we can estimate the assisted signals' instantaneous frequencies that satisfy the relations in TVBF. In our work, we would like to use these traditional tools [1,11] such as Wigner-Ville distribution, pseudo Wigner-Ville distribution, smoothed pseudo Wigner-Ville distribution and short Fourier transform to refine our TFD by fusion rather than some updated TFDs [19,24] because these traditional but simple and reliable TFDs are enough for our task. The fusion procedure is as follow.

1) Calculate the normalized Wigner-Ville distribution $I_{wv}(t, f)$, pseudo Wigner-Ville distribution $I_{pwv}(t, f)$, smoothed pseudo Wigner-Ville distribution $I_{spwv}(t, f)$ and short Fourier transform $I_{sft}(t, f)$. Here the "normalized" means that all the images above are mapped to the value scope between 0 and 1 in proportion.

2) Calculate the first refined TFD by $I_1(t, f) = I_{wv}(t, f) \oplus I_{pwv}(t, f)$, where \oplus denotes

$$I_1(t, f) = I_{wv}(t, f) \oplus I_{pwv}(t, f) = \text{sign}\{I_{wv}(t, f) + I_{pwv}(t, f) - th_1\}$$

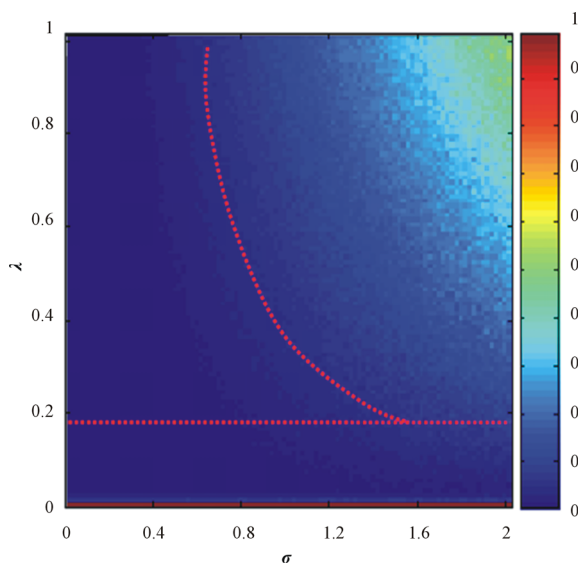


Figure 4. Relation between the error δ with the variance σ and the parameter λ .

(where $\text{sign}(x) = \begin{cases} 1 & x > 0 \\ 0 & \text{else} \end{cases}$) by $th_1 \in [0.1, 0.3]$).

3) Calculate the second refined TFD by

$I_2(t, f) = I_{spwv}(t, f) \oplus I_{sft}(t, f)$ by threshold th_2 (generally $th_2 \in [0.01, 0.2]$). Additional operations: if there are many small isolated regions, then the following steps are adopted: a) perform isolated block removal whose area is less than th_3 (generally $th_3 \in [500, 2000]$) that is the number of the pixels in $I_2(t, f)$; b) dilate the image $I_2(t, f)$; c) erode the image $I_2(t, f)$.

4) Calculate the third refined TFD by

$I_3(t, f) = I_1(t, f) \otimes I_2(t, f)$, where \otimes denotes first performing multiplication pixel by pixel and then the following steps are possibly adopted: a) perform isolated block removal whose area is less than th_4 (generally $th_4 \in [10, 1000]$) that is the number of the pixels; b) dilate the image; c) erode the image.

Note that there is no normal theoretical foundation for the fusion procedure due to the complicated variants in practice. However, these thresholds and the approaches can be found in the similar context in image processing [15]. The similar empirical employment of this fusion procedure can also be found in [19,26].

We find that for most cases, the above procedure plays an effective role in refining the TFD. **Figures 5-7** are three examples showing the effective results by the above procedure. Note that the refining of the TFD in our work is not our final target, which is only a basis in the process of our component separation in noises. Therefore, even we obtain the crude TFD with some distortion in our selected interested regions, if the most pixel points in the true time-frequency ridge are obtained, the effective assisted signals' instantaneous frequencies are available via least squares optimization. For example, in **Figures 5(i)** and **6(i)** there are some points that are not in the true time-frequency ridges, but they are distributed nearly uniformly around the true time-frequency ridges. On the other hand, our assisted signals' instantaneous frequencies can be defined in a scope (see **Figure 4**) limited by λ that give us more tolerance for the distortion of TFD. Similarly, we can select the regions of other interested frequencies in **Figures 5** and **6**. These selected points (t, f) (the red points in the image of **Figures 5(i)** and **6(i)**) can be used to estimate the polynomial instantaneous frequency applied for the construction of assisted signals via least squares optimization.

Since the practical TFDs in noises are possibly too complicated with some intersections, it is too hard to automatically select the interested components' regions in TFDs. Therefore, we have to artificially select our in-

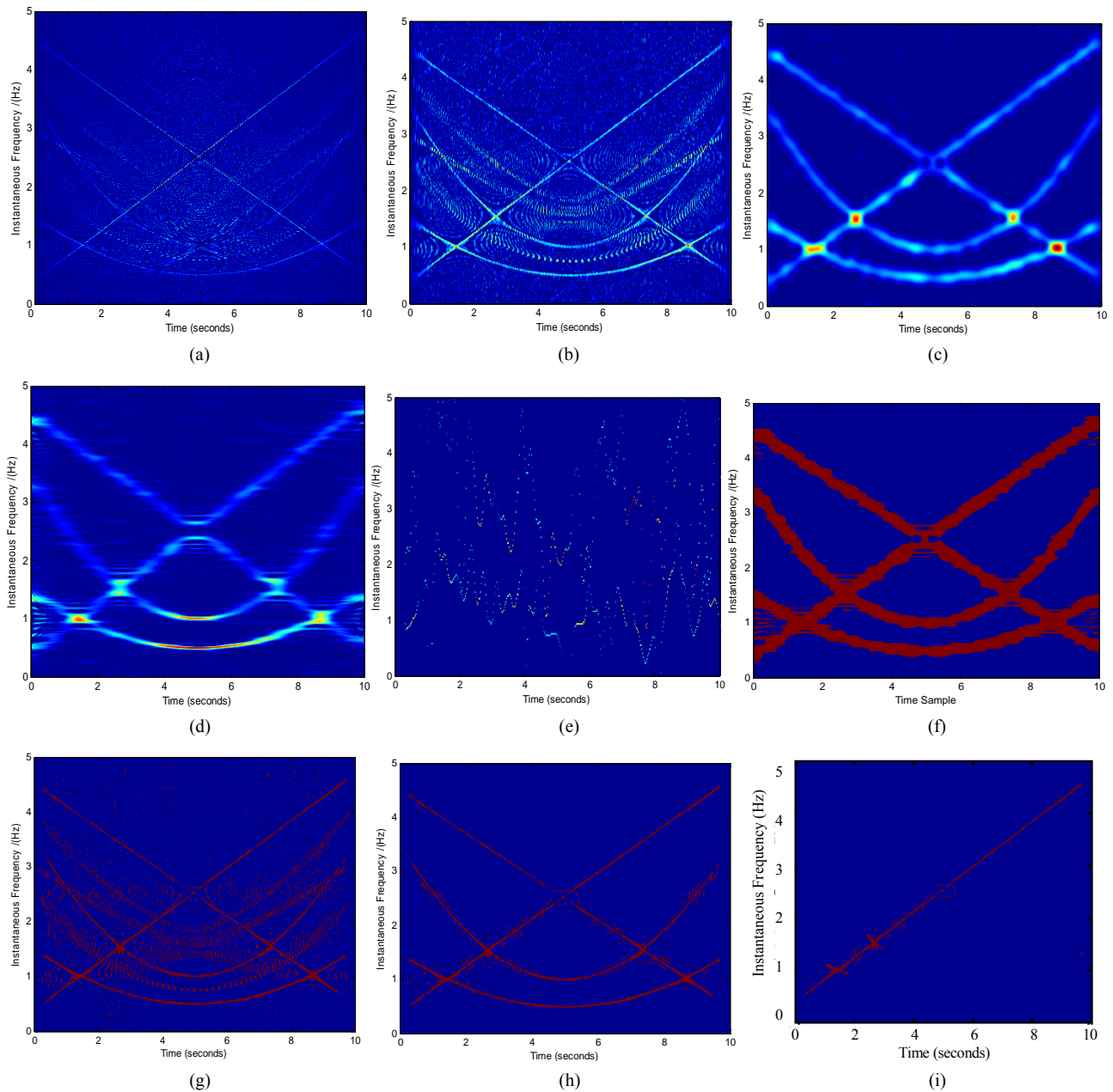


Figure 5. Normalized TFD for assisted instantaneous frequency construction. (a) Wigner-Ville distribution; (b) pseudo Wigner-Ville distribution; (c) short Fourier transform; (d) smoothed pseudo Wigner-Ville distribution; (e) HHT; (f) the fused result of (c) and (d); (g) the fused result of (a) and (b); (h) the fused result of (f) and (g); (i) an example of the interested frequency component selection for the further estimation of assisted signal's instantaneous frequency. Here $th_1 = 0.2$, $x_1(t) = (1 + 0.01t)\cos(2\pi(0.1t^2 - t + 3.5)t)$, $x_2(t) = \cos(2\pi(0.44t + 0.4)t)$, $th_2 = 0.03$, $th_3 = 1000$, $x_3(t) = \cos(2\pi(0.04t^2 - 0.4t + 1.5)t)$, $th_4 = 20$, $x_4(t) = (1 - 0.001t^2)\cos(2\pi(-0.4t + 4.5)t)$, and the zero-mean Gaussian noise's variance $\sigma = 1$. The sampling frequency is 100 Hz.

terested components via image region selection [15]. There are many powerful and skillful tools [15] to help to operate image region selection. Even in MATLAB [9], we can easily operate the image region selection piecewise via some simple tries and tests after a few times.

4.2. Polynomial Instantaneous Frequency Construction via Least Squares

We let the selected region's instantaneous frequency be $f_{in}(t) = \sum_{i=1}^v a_i t^i$ (v is the number of the coefficients).

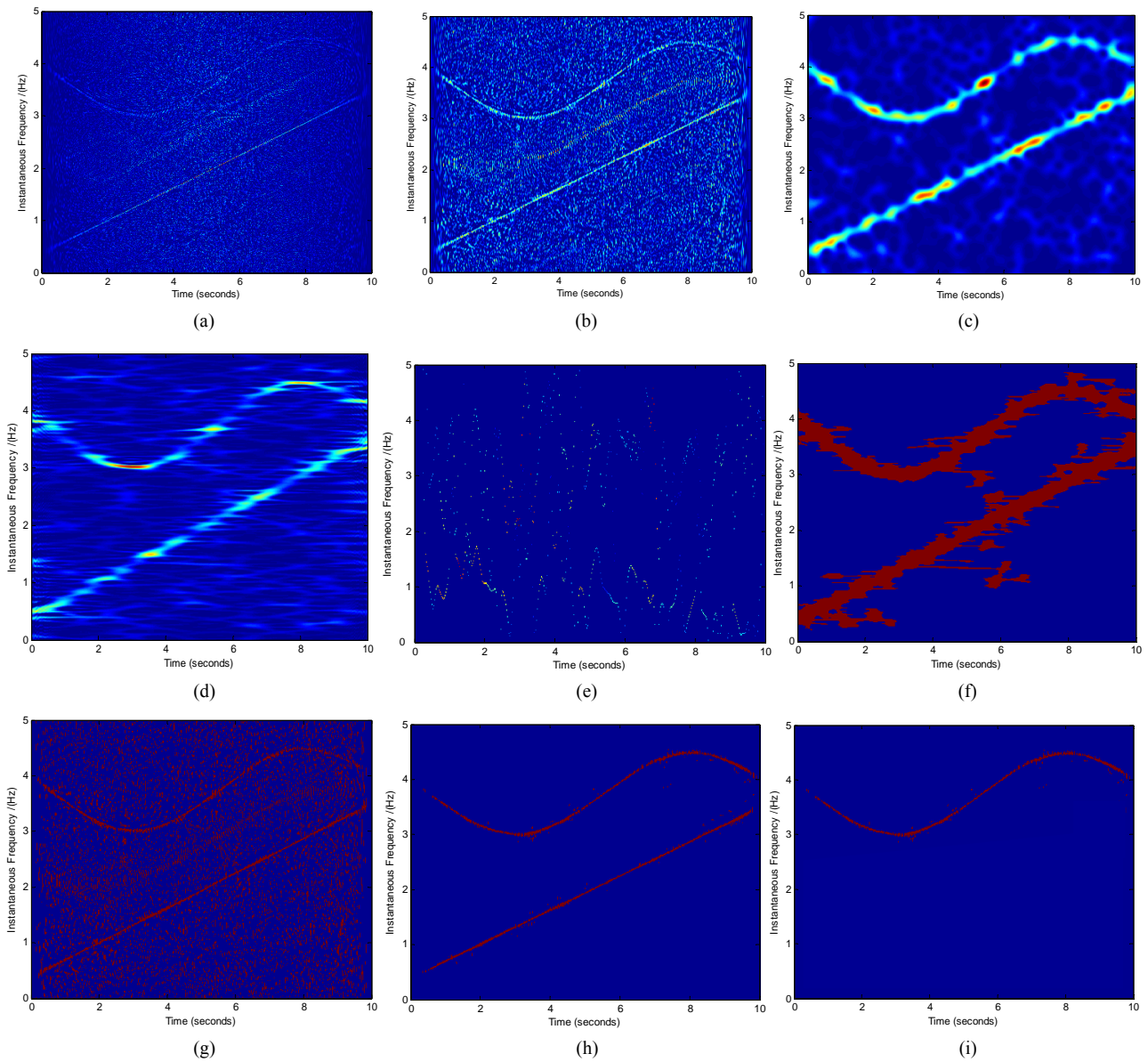


Figure 6. Normalized TFD for assisted instantaneous frequency construction. (a) Wigner-Ville distribution; (b) pseudo Wigner-Ville distribution; (c) short Fourier transform distribution; (d) smoothed pseudo Wigner-Ville distribution; (e) HHT; (f) the fused result of (c) and (d); (g) the fused result of (a) and (b); (h) the fused result of (f) and (g); (i) an example of the interested frequency component selection for the further estimation of assisted signal’s instantaneous frequency. Here $th_1 = 0.2$, $th_2 = 0.03$, $th_3 = 1000$, $x_1(t) = \cos(2\pi(3 - 1.5\sin(0.2\pi t))t)$, $x_2(t) = (0.02t + 1) \cdot \cos(2\pi(0.31t + 0.4)t)$, $th_4 = 20$ and the zero-mean Gaussian noise’s variance $\sigma = \sqrt{2}$. Sampling frequency is 25 Hz.

From the selected region, we can obtain the nonzero pixel points $(t_l, f_{in}(t_l))$ ($1 \leq l \leq L_s \in \mathbb{Z}^+$ and L_s is the number of the nonzero pixel points in the selected region).

$$\text{Set } Y = \begin{bmatrix} f(t_1) \\ f(t_2) \\ \vdots \\ f(t_{L_s}) \end{bmatrix}, A = \begin{bmatrix} a_1 \\ a_2 \\ \vdots \\ a_n \end{bmatrix} \text{ and } B = \begin{bmatrix} 1 & t_1 & t_1^2 & \cdots & t_1^v \\ 1 & t_2 & t_2^2 & \cdots & t_2^v \\ \vdots & \vdots & \vdots & \cdots & \vdots \\ 1 & t_{L_s} & t_{L_s}^2 & \cdots & t_{L_s}^v \end{bmatrix},$$

then we can obtain the optimal parameters via the least squares optimization by

$$A = (B^T B)^{-1} B^T \cdot Y, \tag{18}$$

where the superscript “**T**” is the matrix transpose operator.

In most cases, what we need to do is to provide the number v of the parameters in A . In fact, after the acquisition of the refined TFD, every frequency ridge

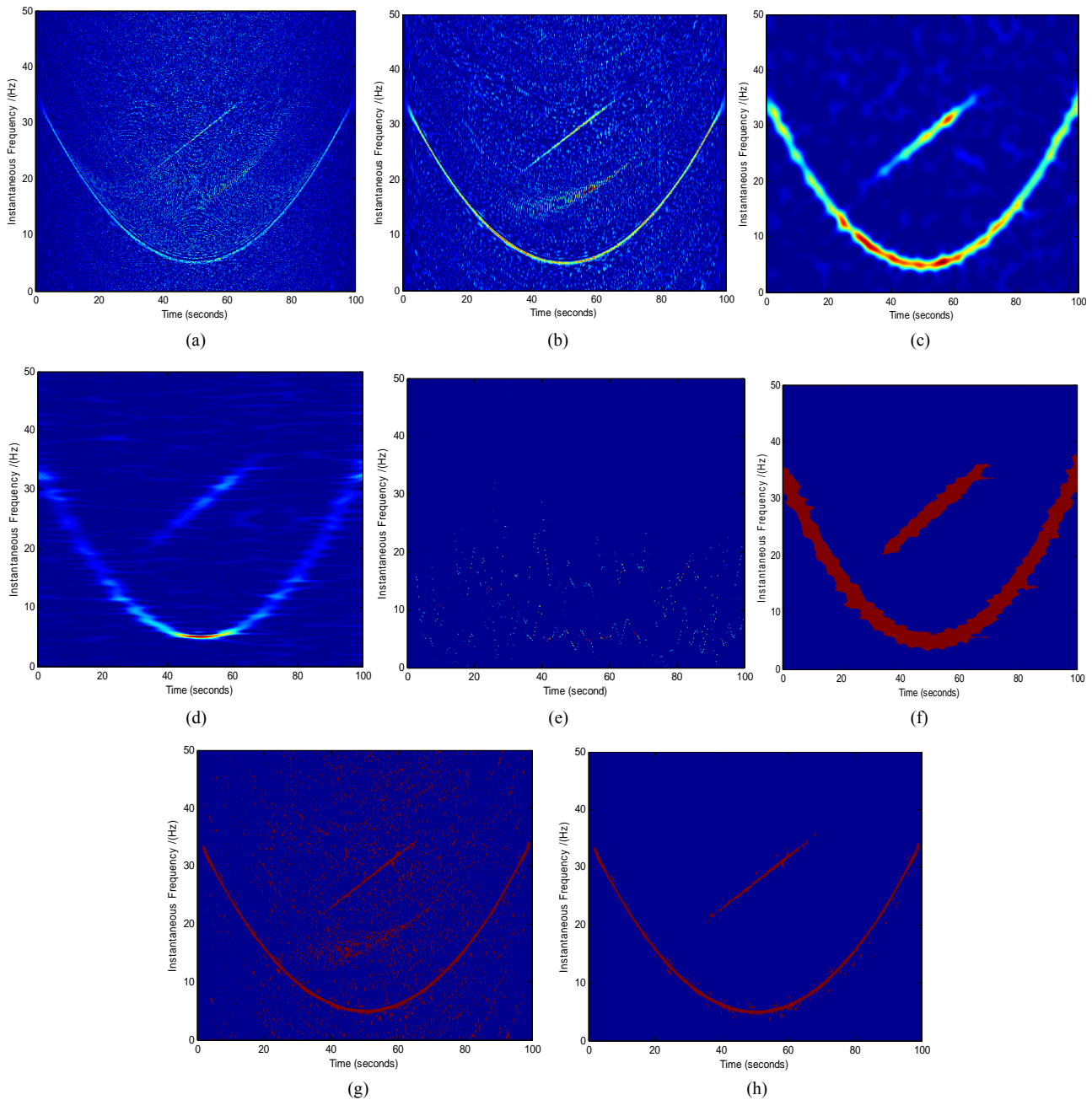


Figure 7. Normalized TFD for assisted instantaneous frequency construction. (a) Wigner-Ville distribution; (b) pseudo Wigner-Ville distribution; (c) short Fourier transform distribution; (d) smoothed pseudo Wigner-Ville distribution; (e) HHT; (f) the fused result of (c) and (d); (g) the fused result of (a) and (b); (h) the fused result of (f) and (g). Here $th_1 = 0.2$, $th_2 = 0.03$, $x_1(t) = 2\cos(2\pi(0.012t^2 - 1.2t + 35)t)$, $x_2(t) = 2e^{-0.003(t-50)^2}\cos(2\pi(0.45t + 5)t)$, $th_3 = 1000$, $th_4 = 20$ and the zero-mean Gaussian noise's variance $\sigma = 1$. The sampling frequency is 250 Hz.

function's shape is salient, and we can give a number a *a priori*. Generally, $v = 5$ works well.

Once the instantaneous frequency $f_{in}(t) = \sum_{i=1}^v a_i t^i$ is determined, we can obtain the according two assisted signals' instantaneous frequencies

$$f_{as,1}(t) = (1 + \lambda) \sum_{i=1}^v a_i t^i \quad \text{and} \quad f_{as,2}(t) = (1 - \lambda) \sum_{i=1}^v a_i t^i$$

to construct the two assisted signal pairs:

$$x_{as,\cos}^{(l)}(t) = \cos(2\pi f_{as,1}(t)t), \quad x_{as,\sin}^{(l)}(t) = \sin(2\pi f_{as,1}(t)t), \quad (19)$$

$$x_{as,cos}^{(2)}(t) = \cos(2\pi f_{as,2}(t)t), x_{as,sin}^{(2)}(t) = \sin(2\pi f_{as,2}(t)t). \tag{20}$$

Furthermore, we can obtain the according interested component's approximation $\tilde{x}_m(t)$ from the noised signal $x(t)$ by

$$\tilde{s}_1(t) = x_{as,sin}^{(1)}(t) \cdot H\{x(t) \cdot x_{as,cos}^{(1)}(t)\} - x_{as,cos}^{(1)}(t) \cdot H\{x(t) \cdot x_{as,sin}^{(1)}(t)\}, \tag{21}$$

$$\tilde{s}_2(t) = x_{as,sin}^{(2)}(t) \cdot H\{x(t) \cdot x_{as,cos}^{(2)}(t)\} - x_{as,cos}^{(2)}(t) \cdot H\{x(t) \cdot x_{as,sin}^{(2)}(t)\}, \tag{22}$$

$$\tilde{x}_m(t) = \tilde{s}_1(t) - \tilde{s}_2(t), \tag{23}$$

and with the SNR

$$snr = 10 \log_{10} \frac{\|x_{in}(t)\|_{L^2(t)}^2}{\|x_{in}(t) - \tilde{x}_m(t)\|_{L^2(t)}^2} = -10 \log_{10} \delta, \tag{24}$$

where $x_{in}(t)$ is the according interested original component.

In practice, the Hilbert transform has the boundary effect [1] near the endpoints that is similar with EMD's boundary effect [20-23]. One of the most used methods [20-23] is the prolonging on the two sides of the original signals via rational extrapolation. Since there are a lot of noises, it is relatively hard to extend the original signals with seamless splicing. Therefore, in this work we use one simple but effective method: mirror extension [20]. We find that although the mirror extension cannot eliminate the boundary effect completely, it greatly attenuates the errors resulted by the boundary effect.

5. Experiments and Discussion

5.1. On Simulations

In this section, we will use the proposed method to sepa-

rate the noised AM-FM components in the **Figures 5-7**. There are eight significant AM-FM components at all. In these experiments, we take $\lambda = 0.02$ for all components. The compared methods include the empirical mode decomposition (EMD) [12], the improved EMD (IEMD) [2], the Hilbert transform based method [16] via Fourier spectra, the masking method [13,14] and our proposed method. In EMD we will use the most related IMF to the original true component as the according separated component. In IEMD and the masking method, we first perform simple filtering by EMD via discarding the first two IMFs. In the Hilbert transform based method [16], we assume the number of the components in noises is known so that we can obtain according modes' number *a priori*. The comparison via SNR can be found in **Table 1**. The measure used in **Table 1** is defined in (24). The signals that are decomposed come from **Figures 5-7**. The comparison methods are the above mentioned methods: EMD, IEMD, masking method and our proposed method.

One notation is that all the other four methods (EMD, IEMD, masking method and the Hilbert transform based method [16]) fail to separate the components with crossed instantaneous frequencies. EMD, IEMD and masking method only extract the high-frequency part every time. At the same time, they are seriously affected by the noises. The method [16] employs the Fourier spectra to obtain the assisted signals' constant frequencies, which are not suitable for the time-varying frequency components, and in other words, it only holds for the components with distinguishable (or non-overlapped) frequency regions in Fourier spectra. Therefore, these four methods' performance is far lower than our proposed method for the more general and complicated cases in noises.

In **Figure 7**, the second component $x_2(t)$ is intermittent. In this case, we still obtain the selected region including the according pixels that are related with the instantaneous frequency of $x_2(t)$ at first. Then the construction of the assisted signals is also the same as that of

Table 1. The comparison between some methods to separate the components in noises.

	snr							
	Figure 5				Figure 6		Figure 7	
	$x_1(t)$	$x_2(t)$	$x_3(t)$	$x_4(t)$	$x_1(t)$	$x_2(t)$	$x_1(t)$	$x_2(t)$
EMD [3]	1.2574	1.0001	-	3.4464	2.2574	2.3072	1.8894	-
IEMD [6]	-	-	4.3375	5.1247	4.1113	3.8879	-	-
Masking method [4,5]	3.6905	-	2.3467	2.9870	3.9802	-	6.4301	-
Method in [2]	3.8979	3.7021	2.2554	-	6.8794	3.3210	7.2578	-
Our method	17.1615	18.4958	21.7105	14.6292	15.2934	14.3257	17.5273	19.3419

Here “-” denotes this term is negative.

non-intermittent component. The difference is the extraction of the component using TVBF. Since the component is intermittent, then its effective time support is short than the whole time support. Therefore, we only need to extract the according component in the effective time support that can be estimated in the refined TFD. In order to reduce the lose of the small instantaneous amplitude as much as possible without introducing more noises, we can extract the component by

$$\tilde{x}_m(t) = \begin{cases} \tilde{s}_1(t) - \tilde{s}_2(t), & t_1 - \Delta t \leq t \leq t_2 + \Delta t \\ 0, & \text{elsewhere} \end{cases}, \quad (25)$$

where $[t_1, t_2]$ is the component's effective time support roughly estimated in the TFD, and here we take $\Delta t = (t_2 - t_1)/4$.

Another problem is the sampling frequency. Since Hilbert transform will be affected by the sampling frequency and the signal's max frequency, we must take into account the ratio between the sampling frequency and the signal's max frequency. We find that with the increasing of the ratio between the sampling frequency and the signal's max frequency, the performance will upgrade, and vice versa. **Figure 8** is the relation between the SNR and the frequency ratio for the separation of the two components from **Figure 6**. We find that the higher the ratio, the higher the SNR. In addition, when the ratio is more than 10, the SNR varies slowly. In the same manner, we also test the components in **Figures 5** and **7** and obtain the same conclusion for fixed noise's variance: when the ratio is more than about 10, the performance is better. On the other hand, when the ratio is more than about 5, the performance is nearly acceptable.

5.2. Experiments on Real-Life Data of Bat

In this section, we will use the proposed method to ana-

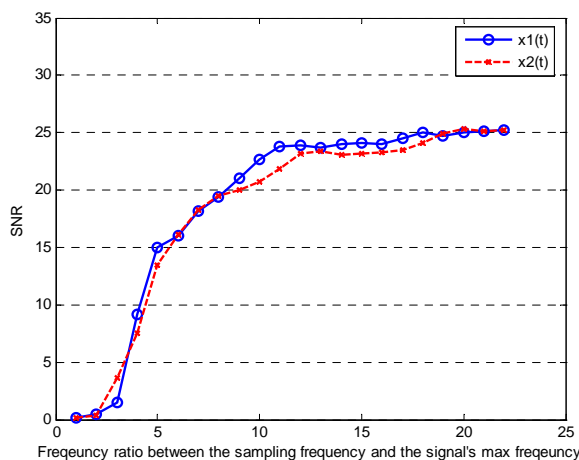


Figure 8. The relation between SNR and the frequency ratio for the two components from **Figure 6**.

lyze the noised bat's data (see **Figure 9(a)**). Since the data is disturbed by heavy noises, the true components in the data cannot be seen at all. Now we compared some methods with our proposed method to separate them. The compared methods include the empirical mode decomposition (EMD) [12] and the improved EMD (IEMD) [2]. IEMD cannot find the according assisted component and it fails to do this work because of the heavy noises (so there is no according result here). EMD can do this work, but its result (see **Figure 9(f)**) has no physical sense from the real-life nature. Instead, since our method makes full use of the fused time-frequency distribution and the function of soft-cutting in frequency domain, we finally obtain the two main decomposed components (see **Figures 9(j)** and **(k)**) with its rational physical interpretation (see **Figure 9(i)**).

6. Conclusions

AM-FM signals are widely used in various signal processing fields. When multiple AM-FM components are blended in noises, how to separate them is still a challenge. The tasks in the separation of multiple AM-FM components blended in noises are twofold: one is the denoising and another is the decomposition of these components. Especially when the frequency spectra of these components have overlapped regions in Fourier transform domain and even their instantaneous frequencies have crossed points in TFD, how to extract every AM-FM component is nearly an open question to our knowledge. In this paper, we merge the two tasks (filtering the noises and decomposition of these components) to one new derived method.

Our contribution mainly includes the following. First, the Hilbert transform based decomposition is analyzed for the time-varying frequency components (*i.e.*, nonstationary signals) via representative simulations and theoretical analyses. From these simulations and analyses we can obtain the conclusion: this method holds for the complicated case that the components have overlapped frequency regions in transform domain, which is a breakthrough in decomposing noised signals so that this demonstrates great potential valuable performance in the separation of components for more general/complicated cases. Second, based on the above analysis, a hypothesis with the condition that AM-FM components can be separated successfully based on Hilbert transform and the assisted signal is proposed, which is supported by the experiments. After this, the time-varying bandpass filter (TVBF) based on assisted signals is proposed to separate the components blended in noises. The assisted signals used in TVBF are derived from the refined TFDs via image fusion and least squares optimization. The theoretical errors are also analyzed to bound the performance

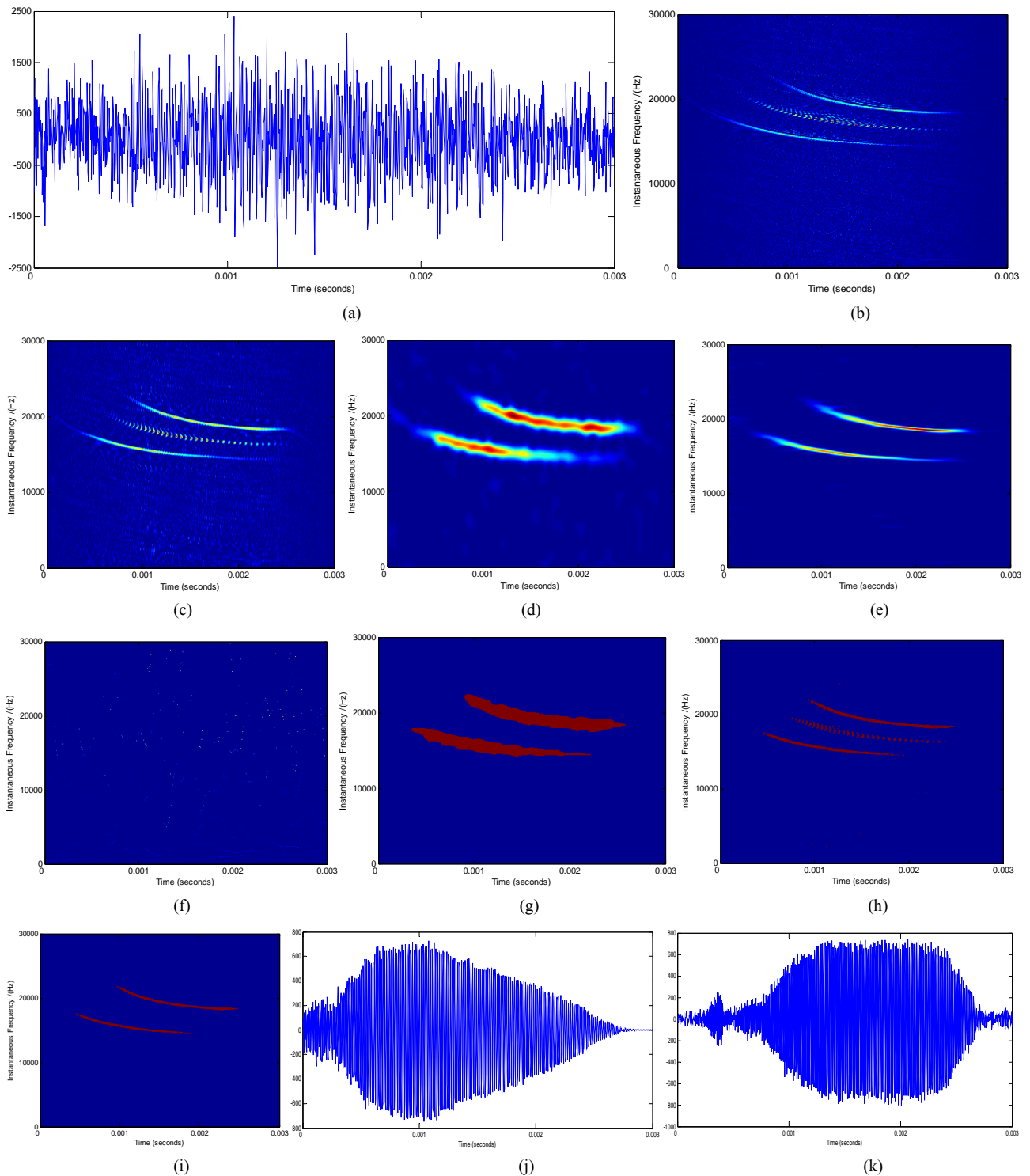


Figure 9. The analysis of real-life data of bat. (a) The noised real-life data of bat; (b) Wigner-Ville distribution; (c) pseudo Wigner-Ville distribution; (d) short Fourier transform distribution; (e) smoothed pseudo Wigner-Ville distribution; (f) HHT; (g) the fused result of (d) and (e); (h) the fused result of (b) and (c); (i) the fused result of (g) and (h); (j) the first component separated by our method; (k) the second component separated by our method.

of this method: the error is proportional to the product of the two parameters: λ and σ^2 . Finally, some representative experiments on man-made and real-life data are

shown to verify the efficiency of the proposed method and demonstrate the advantages over the other main methods.

Our biggest contribution of this paper is that we introduce a novel approach filtering and decomposing signals in a fully different manner. Our proposed TVBF seems like a “soft-cutter” and expediently cuts the components that have complicated instantaneous frequencies in frequency domain with rational physical sense. This method changes the idea of filtering and decomposing signals and will be a breakthrough from “soft” filtering and decomposing signals. In addition, one of our method’s biggest advantages is that we merge the two tasks (filtering and decomposing) to single one, which effectively separates the components blended in noises that other methods fail to do.

REFERENCES

- [1] X. D. Zhang, “Modern Signal Processing,” 2nd Edition, Tsinghua University Press, Beijing, 2002.
- [2] G. Xu, X. Wang and X. Xu, “Time-Varying Frequency-Shifting Signal Assisted Empirical Mode Decomposition Method for AM-FM Signals,” *Mechanical Systems and Signal Processing*, Vol. 23, No. 8, 2009, pp. 2458-2469. [doi:10.1016/j.ymssp.2009.06.006](https://doi.org/10.1016/j.ymssp.2009.06.006)
- [3] A. O. Boudraa and J. C. Cexus, “EMD-Based Signal Filtering,” *IEEE Transactions on Instrumentation and Measurement*, Vol. 56, No. 6, 2007, pp. 2196-2202. [doi:10.1109/TIM.2007.907967](https://doi.org/10.1109/TIM.2007.907967)
- [4] J. G. Proakis and D. G. Manolakis, “Digital Signal Processing: Principles, Algorithms, and Applications,” 3rd Edition, Prentice-Hall, Englewood Cliffs, 1996.
- [5] D. L. Donoho and I. M. Johnstone, “Ideal Spatial Adaptation via Wavelet Shrinkage,” *Biometrika*, Vol. 81, 1994, pp. 425-455. [doi:10.1109/18.382009](https://doi.org/10.1109/18.382009)
- [6] D. L. Donoho, “De-Noising by Soft-Thresholding,” *IEEE Transactions on Information Theory*, Vol. 41, No. 3, 1995, pp. 613-627.
- [7] S. Mallat and Z. Zhang, “Matching Pursuits with Time-Frequency Dictionaries,” *IEEE Transactions on Signal Processing*, Vol. 41, No. 12, 1993, pp. 3397-3415. [doi:10.1109/78.258082](https://doi.org/10.1109/78.258082)
- [8] G. L. Xu, X. T. Wang, X. G. Xu and L. J. Zhou, “Improved EMD for the Analysis of FM Signals,” *Mechanical Systems and Signal Processing*, Vol. 33, No. 11, 2012, pp. 181-196. [doi:10.1016/j.ymssp.2012.07.003](https://doi.org/10.1016/j.ymssp.2012.07.003)
- [9] F. Auger, P. Flandrin and P. Gonçalves, “Time-Frequency in Action with Matlab,” 2000. http://www.researchgate.net/publication/50207277_Time-frequency_in_action_with_Matlab
- [10] B. Boashash, “Time-Frequency Signal Analysis and Processing—A Comprehensive Reference,” Elsevier Science, Oxford, 2003.
- [11] L. Cohen, “Time-Frequency Analysis,” Prentice-Hall, New York, 1995.
- [12] N. E. Huang, S. Zheng, R. L. Steven, *et al.*, “The Empirical Mode Decomposition and the Hilbert Spectrum for Nonlinear Non-Stationary Time Series Analysis,” *Proceedings of the Royal Society A*, Vol. 454, 1998, pp. 903-995. [doi:10.1098/rspa.1998.0193](https://doi.org/10.1098/rspa.1998.0193)
- [13] R. Deering and J. F. Kaiser, “The Use of a Masking Signal to Improve Empirical Mode Decomposition,” *IEEE International Conference on Acoustics, Speech, and Signal Processing*, Vol. 4, 2005, pp. IV485- IV488.
- [14] N. Senroy, S. Suryanarayanan and P. F. Ribeiro, “An Improved Hilbert-Huang Method for Analysis of Time-Varying Waveforms in Power Quality,” *IEEE Transactions on Power Systems*, Vol. 22, No. 4, 2007, pp. 1843-1850. [doi:10.1109/TPWRS.2007.907542](https://doi.org/10.1109/TPWRS.2007.907542)
- [15] C. R. Gonzalez and E. R. Woods, “Digital Image Processing,” Pearson Education, 2nd Edition, Prentice Hall Press, Upper Saddle River, 2003.
- [16] G. Chen and Z. Wang, “A Signal Decomposition Theorem with Hilbert Transform and Its Application to Narrowband Time Series with Closely Spaced Frequency Components,” *Mechanical Systems and Signal Processing*, Vol. 28, 2012, pp. 258-279. [doi:10.1016/j.ymssp.2011.02.002](https://doi.org/10.1016/j.ymssp.2011.02.002)
- [17] R. Tao, B. Deng and Y. Wang, “Theory and Application of the Fractional Fourier Transform,” Tsinghua University Press, Beijing, 2009.
- [18] G. Rilling and P. Flandrin, “One or Two Frequencies? The Empirical Mode Decomposition Answers,” *IEEE Transactions on Signal Processing*, Vol. 56, No. 1, 2008, pp. 85-95. [doi:10.1109/TSP.2007.906771](https://doi.org/10.1109/TSP.2007.906771)
- [19] L. Angrisani, M. D’Arco, R. S. Lo Moriello, *et al.*, “On the Use of the Warble Transform for Instantaneous Frequency Estimation,” *IEEE Transactions on Instrumentation and Measurement*, Vol. 54, No. 4, 2005, pp. 1374-1380. [doi:10.1109/TIM.2005.851060](https://doi.org/10.1109/TIM.2005.851060)
- [20] J. P. Zhao and D. J. Huang, “Mirror Extending and Circular Spline Function for Empirical Mode Decomposition Method,” *Journal of Zhejiang University Science*, Vol. 2, No. 3, 2001, pp. 247-252. [doi:10.1631/jzus.2001.0247](https://doi.org/10.1631/jzus.2001.0247)
- [21] Y. J. Deng, *et al.*, “An Approach for Ends Issue in EMD Method and Hilbert Transform,” *Chinese Science Bulletin*, Vol. 46, No. 3, 2001, pp. 903-1005.
- [22] J. Cheng, D. Yu and Y. Yang, “Discussion of the End Effects in Hilbert-Huang Transform,” *Journal of Vibration and Shock*, Vol. 24, No. 6, 2005, pp. 40-47.
- [23] J. Wang, Y. Peng and X. Peng, “Similarity Searching Based Boundary Effect Processing Method for Empirical Mode Decomposition,” *Electronics Letters*, Vol. 43, No. 1, 2007, pp. 1-2.
- [24] Y. Yang, W. M. Zhang, Z. K. Peng and G. Meng, “Time-Frequency Fusion Based on Polynomial Chirplet Transform for Non-Stationary Signals,” *IEEE Transactions on Industrial Electronics*, Vol. 60, No. 9, 2012, pp. 3948-3956. [doi:10.1109/TIE.2012.2206331](https://doi.org/10.1109/TIE.2012.2206331)
- [25] E. Bedrosian, “A Product Theorem for Hilbert Transforms,” Memorandum RM-3439-PR, US Air Force Project RAND, 1962.